

금 나노 입자의 전하 구속을 이용한 실리콘 기반 웨어러블 비휘발성 메모리 어레이

김재민, 손동희, 이민철, 김대형

기초과학연구원 나노입자 연구단, 서울대학교 화학생물공학부

## **Wearable Silicon Based Nonvolatile Memory Array Using Nanocrystal Charge Confinement**

Jaemin Kim, Donghee Son, Mincheol Lee, Dae-Hyeong Kim

Center for Nanoparticle Research, Institute for Basic Science  
School of Chemical and Biological Engineering, Seoul National University

### 서론

Flash memory based on the single crystal silicon (Si) is a dominating nonvolatile data storage device due to its high performance and compatibility with complementary metal–oxide–semiconductor (CMOS) processes<sup>1</sup>. Various studies on new materials to replace conventional floating gates (FGs) toward the enhancement of charge storage efficiency have been reported. However, FGs using conducting thin films have challenging issues, such as difficulties in modulation of charge trap density and charge losses via locally distributed defects in surrounding dielectric<sup>2</sup>. As a viable alternative, gold nanoparticles (AuNPs) FG has been highlighted. AuNP FGs have many advantages, such as controllability of the charge trap density, superb chemical stability, high work function, and most importantly, efficient charge confinement<sup>3</sup>. However, detailed nanoscale experimental observations of charge confinement in closely packed AuNP FGs and relevant device characterizations has not been reported yet.

Meanwhile, the rapid expansion of wearable electronics brings immediate needs to develop deformable electronic devices. Even though stretchable Si diodes, transistors, sensors, and logic circuits have been reported, the deformable charge trap FG memory (CTFM) based on single crystal Si is not studied. Their integration with other sensors and electronics in one wearable platform is another important goal to accomplish. In pursuit of the large memory window and capacity with the high cell-to-cell uniformity, the efficient fabrication process for the uniform and high density assembly of AuNPs over the large area is also a key requirement.

Here, we develop high-density wearable Si nanomembrane (SiNM) CTFMs with the FG of AuNPs assembled by the Langmuir-Blodgett (LB) method. The particle-wise charge confinement without charge delocalization in closely packed AuNPs is confirmed, which leads to the long retention time. LB assembly enables the large memory window and high cell-to-cell uniformity. The CTFM array is multiplexed for the individual addressing and data storage. The ultrathin and stretchable form of CTFMs allows conformal lamination on the skin. By interfacing with wearable Si amplifiers and electrodes, constantly recovering heart rates are measured after exercise stress tests and the recorded data are stored in CTFMs, which are retrieved later for the diagnosis of cardiovascular autonomic dysfunction.

### 실험결과

A FG cell (FGC; insulator-FG-insulator-semiconductor structure) is fabricated to verify nanoscale charge confinement in a closely packed AuNPs FG. The conductive atomic force microscopy (AFM) tip with applied potential of 7 V contacts the top insulation layer of the FGC (blocking oxide; B<sub>ox</sub>) and injects charges following predetermined patterns (Fig. 1a). The potential difference between the AFM tip and the bottom Si substrate facilitates trapping of electrons to AuNPs FG (Fig. 1a inset). A series of AFM writings finish the patterned charge injection.

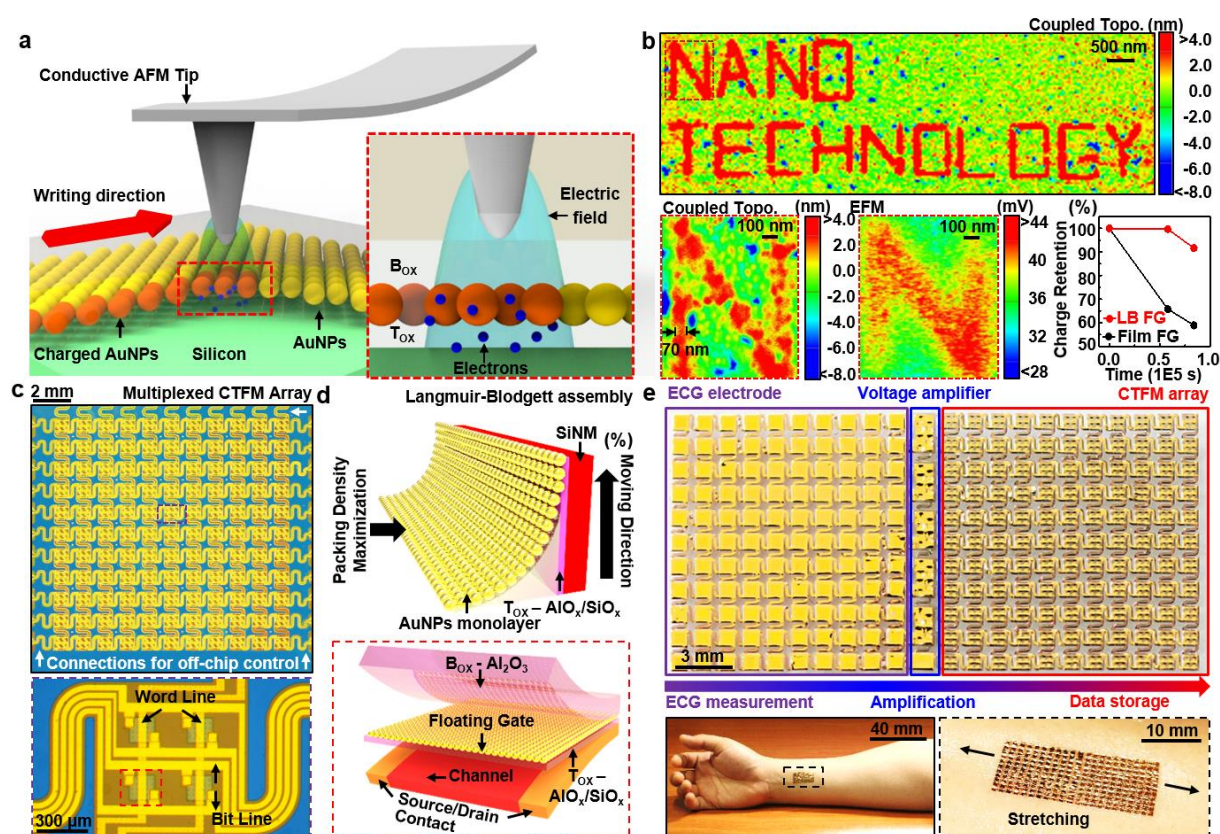


**Figure 1 | Large-area assembly of AuNPs for system-level demonstration of nonvolatile memory array**

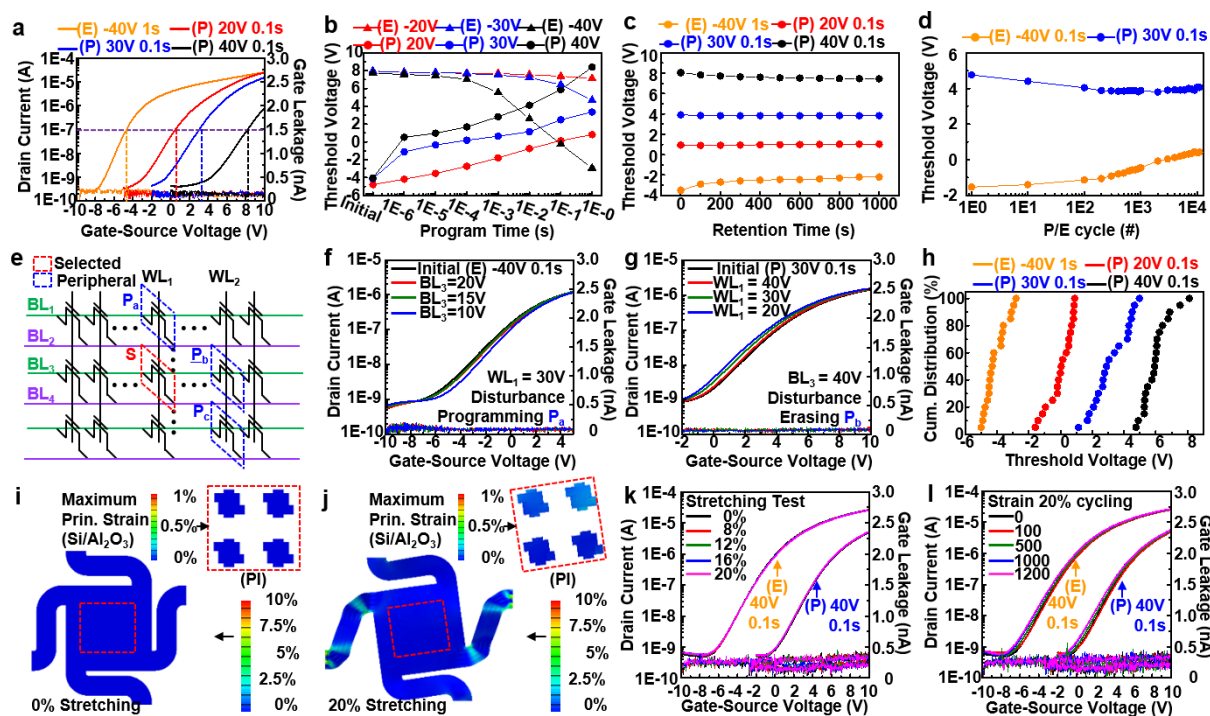
The nanoscale charge confinement in FG is characterized by the modified AFM measurement. The local electric force produced by confined charges (electric force microscopy; EFM) is coupled with topographical AFM data to see the charge pattern (Fig. 1b top). In contrast to the blurred EFM image, the coupled image clearly shows the nanoscale charge confinement ( $\sim 70$  nm line width) with no lateral charge transport (Fig. 1 bottom left and middle). We additionally compared the retention property of the AuNPs FG to those of the conventional metal (Au) film FG (Fig. 1b bottom right). The AuNPs FG shows superior performance to the Au film FG. The efficient charge confinement of AuNPs leads to CTFMs of the long retention time.

Figure 1c exhibits the photograph of a  $22 \times 22$  multiplexed CTFM array (top) and its magnified view showing four CTFMs (bottom). All CTFMs in the array are based on silicon transistors and fully multiplexed, individually accessed, and readily programmed, erased, and read by the off-chip control. The LB assembly capability that successfully fabricates a closely packed AuNPs FG over large area (Fig. 1d) guarantees the high uniformity of CTFM performances. The AuNPs FG is located between the tunneling oxide ( $T_{ox}$ ) and  $B_{ox}$  (Fig. 1d bottom).

Figure 1e shows a wearable platform of the CTFM array (top right) with stretchable electrodes (top left) and voltage amplifiers (top middle). The amplifier is composed of silicon pseudo CMOS inverters. Electrocardiogram (ECG) is measured (electrodes), amplified (amplifiers), and stored (CTFMs) on the skin. Its ultrathin structure ( $\sim 5$   $\mu\text{m}$ ) and serpentine interconnects enable its conformal lamination on the human skin under stretched states (Fig. 1e bottom). The single crystal nature of silicon provides high performances in electronics and the multiplexed memory array.

The electrical characteristics of the fabricated CTFM array transferred on the stretchable substrate are evaluated by addressing to the each memory pixel. Figure 2a depicts transfer characteristics of a CTFM showing multi-level-cell (MLC) operation capability. As the amplitude of PGM/ERS pulse increases, the threshold voltage ( $V_{th}$ , indicated with dotted lines in Fig. 2a) shifts

further. PGM/ERS speed characteristics of the CTFM also show that the  $V_{th}$  is depending on the amplitude of the PGM/ERS pulse, as well as on the duration of the PGM/ERS pulse (Fig. 2b). Figure 2c shows stably retained multiple states stored in the CTFM pixel. The electrical verification of the states stored in the CTFM pixel is still available even after multiple PGM/ERS cycles up to  $10^4$  cycles (Fig. 2d).



**Figure 2 | Electrical and mechanical characterization of CTFM array**

Figure 2e shows the schematic of the CTFM array in a NOR-type configuration. We investigated electrical disturbances between selected (S, red box) and peripheral ( $P_a$ - $P_c$ , blue box) memory pixels. Once the pixel S is erased/programmed, the co-applied inhibition pulse on bit line (BL)/word line (WL) can prevent severe change of the stored state during the PGM/ERS operations of the peripheral pixels (Fig. 2f and g). Cumulative probability data of each level obtained from the multiple memory pixels show that the MLC operation works well in the CTFM array (Fig. 2h). Slightly nonuniform  $V_{th}$  distribution might be originated from difference in interconnects resistance of near and far memory pixels.

To characterize the reliability of the CTFM during the mechanical deformation, the CTFM array has been under the stretching test. The finite element analysis (FEA) results show that memory pixels in red dotted box region undergo negligible strains ( $\sim 0.2\%$ , cf. fracture strain of Si :  $\sim 1\%$ ;  $Al_2O_3$  :  $\sim 2\%$ ) while the CTFM array is stretched by 20%, facilitated by serpentine interconnects accommodating most of the applied strain (Fig. 2i and j). The PGM/ERS operations of the CTFM are conducted under various degrees of the deformation (Fig. 2k) and after multiple stretching cycles up to 1200 cycles with 20% strain (Fig. 2l). In both tests, minimal performance degradation has been observed. Considering that the strain limitation of human epidermis is  $\sim 20\%$ , the excellent mechanical reliability paves the way for the application of the CTFM in wearable and stretchable system.

Figure 3a illustrates the procedures of the demonstration. The procedures are composed of ECG signals acquisition, on-site amplification, heart rate measurement, data storage/retrieve to/from the CTFM array, in sequence. The data comprised of the heart rate and elapsed time are converted to binary number and row-wisely stored in the CTFM array (Fig. 3b). Both the number of peaks and elapsed time data occupy eight memory pixels, respectively, thereby allowing their maximum storable values bound to 255. The amplified ECG signals measured by wearable electrodes and commercial electrodes are depicted in Fig. 3c. Using the wearable electrodes and amplifier, volunteer's heart rates

after the halt of exercise are monitored (Fig. 3d). We first apply PGM/ERS pulses to the selected row of the CTFM array to store the heart rate recovery data illustrated in Fig. 3d. The stored data are read out from the CTFM array right after the data storage and its map is shown in Fig. 3e. The stored data are read out after six hours, showing the good retention property of the CTFM array (Fig. 3f). White boxes indicate erased memory pixels storing a binary number of '0', and black boxes indicate programmed memory pixels storing a binary number of '1'. The stored data contains heart rate and elapsed time encoded with binary number and can be easily converted to decimal number to check the wearer's heart rate recovery history by a medical personnel.

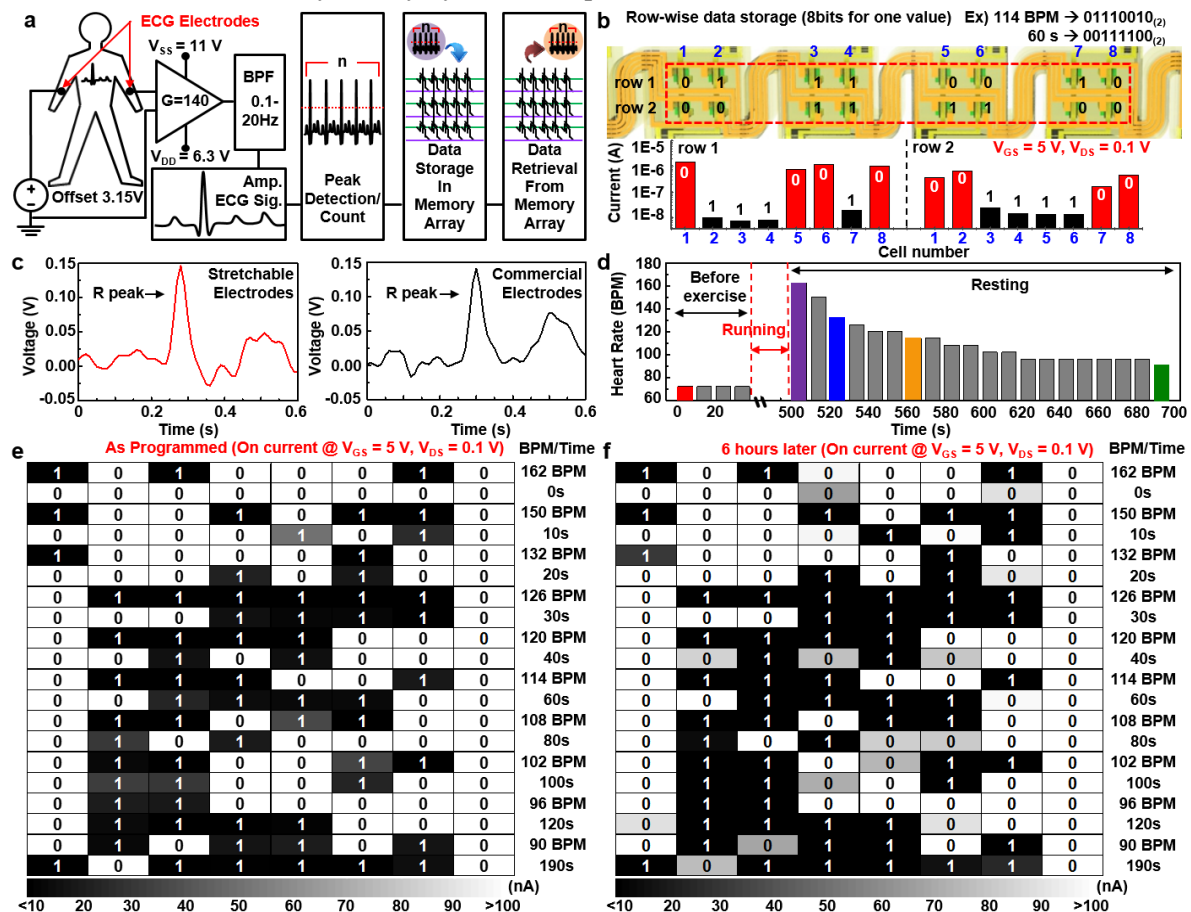


Figure 3 | ECG signal acquisition and storage of information of heart rate recovery

## 토론

The proposed SiNM based CTFM array of LB-assembled AuNPs FG, integrated with additional advanced silicon electronics and sensors in stretchable layout will potentially facilitate the stable storage of the medically useful bio signals processed by integrated electronics for time-delayed or remote diagnosis of diseases.

## 참고문헌

1. Bez, R., Camerlenghi, E., Modelli, A. & Visconti, A. Introduction to flash memory. *Proc. IEEE* 91, 489–502 (2003).
2. Lee, J.-S. Recent progress in gold nanoparticle-based non-volatile memory devices. *Gold Bull.* 43, 189–199 (2010).
3. Lee, J.-S. *et al.* Layer-by-layer assembled charge-trap memory devices with adjustable electronic properties. *Nature Nanotech.* 2, 790–795 (2007).